

Configurational and Conformational Analysis of Chiral Molecules Using IR and VCD Spectroscopies: Spiropentylcarboxylic Acid Methyl Ester and Spiropentyl Acetate

F. J. Devlin,[†] P. J. Stephens,^{*,†} C. Österle,[‡] K. B. Wiberg,[‡] J. R. Cheeseman,[§] and M. J. Frisch[§]

Department of Chemistry, University of Southern California, Los Angeles, California 90089-0482,
Department of Chemistry, Yale University, New Haven, Connecticut 06511, and Gaussian Inc.,
140 Washington Avenue, North Haven, Connecticut 06473

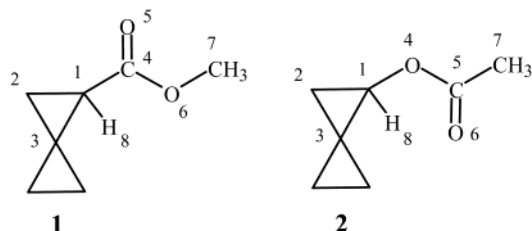
stephens_pj@hotmail.com; pstephen@usc.edu

Received April 2, 2002

The chiral monosubstituted derivatives of spiropentane, spiropentylcarboxylic acid methyl ester, **1**, and spiropentyl acetate, **2**, have been synthesized in optically active form. Configurational and conformational analysis of **1** and **2** has been carried out using infrared (IR) and vibrational circular dichroism (VCD) spectroscopies. Analysis of the experimental IR and VCD spectra has been carried out using ab initio density functional theory (DFT). For both **1** and **2**, DFT predicts two populated conformations. Comparison to experiment of the conformationally averaged IR and VCD spectra of **1** and **2**, predicted using DFT, provides unequivocal evidence of the predicted conformations and yields the absolute configurations *R*(-)/*S*(+) for **1** and *R*(+)/*S*(-) for **2**. These absolute configurations are consistent with the *R*(-)/*S*(+) absolute configuration of spiropentylcarboxylic acid, assigned previously via X-ray crystallography of its α -phenylethylammonium salt.

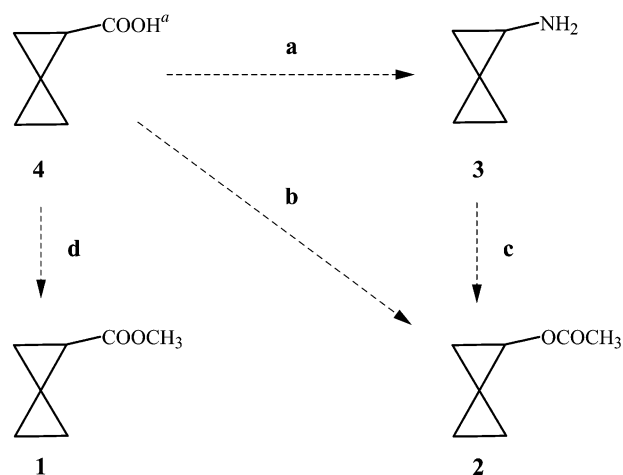
Introduction

We report the configurational and conformational analysis of two chiral derivatives of spiropentane, spiropentyl carboxylic acid methyl ester, **1**, and spiropentyl acetate, **2**, using vibrational unpolarized absorption (infrared (IR)) and vibrational circular dichroism (VCD) spectroscopies.



The stereochemistry and mechanism of the nitrous acid deamination of spiropentylamine in acetic acid was recently studied.¹ Optically active spiropentylamine, **3**, and spiropentyl acetate, **2**, of known relative configurations were prepared from optically active spiropentylcarboxylic acid, **4**, using reactions of known stereochemistry (Scheme 1), and the specific rotations of **2** and **3** established. Measurement of the specific rotation of **2** obtained by deamination of optically active **3** then led to

SCHEME 1^a



^a Reagents and conditions: (a) Curtius reaction; (b) MeLi, urea/H₂O₂ and (CF₃CO)₂O; (c) HNO₂ in CH₃COOH; (d) CH₂N₂.

the conclusion that deamination occurs with essentially complete inversion of configuration, consistent with S_N2 displacement at a spiropentyl diazonium ion intermediate. Simultaneously, the absolute configuration (AC) of **4** was determined via X-ray crystallography of its salt with (*S*)-(-)- α -phenylethylamine to be *R*(-)/*S*(+).¹ This in turn allowed the ACs of **2** and **3** to be inferred: **2**, *R*(+)/*S*(-); **3**, *R*(-)/*S*(+). The determination of the AC of **4** from the X-ray structure of its α -phenylethylammonium salt requires the discrimination of the isoelectronic CH₃ and NH₃⁺ groups of the α -phenylethylammonium ion. One of these groups is adjacent to the COO⁻ group of a spiro-

* To whom correspondence should be addressed. Fax: (213) 740-3792.

[†] University of Southern California.

[‡] Yale University.

[§] Gaussian Inc.

(1) Wiberg, K. B.; Österle, C. *J. Org. Chem.* **1999**, *64*, 7763.

pentylcarboxylate ion and was identified as NH_3^+ on the basis of an interatomic distance.

Since the ACs of monosubstituted spiropentyl derivatives have not otherwise been reported, it is clearly important to confirm the correctness of the ACs of **2**, **3**, and **4** assigned previously. In this work we reexamine the ACs of two of these compounds, **2** and **4**, using VCD spectroscopy.² **2** has been studied directly; in the case of **4**, we have studied its methyl ester derivative, **1**. The determination of the AC of a sample of a chiral molecule using VCD proceeds as follows.³ The IR spectrum is measured and assigned on the basis of the IR spectrum predicted using ab initio density functional theory (DFT). The VCD spectrum is then measured for a sample of known optical rotation and calculated using ab initio DFT. Comparison of the signs of the VCD observed for unambiguously assigned bands in the IR spectrum to the signs calculated using DFT for both enantiomers leads to the AC of the experimental sample. In the case of conformationally flexible molecules, the IR and VCD spectra are the population-weighted sum of the spectra of the individual conformations. Conformational analysis is thus an integral part of the configurational analysis procedure. The molecules **1** and **2** are conformationally flexible: multiple conformations of the ester group in **1** and of the acetate group in **2** relative to the spiropentyl group are possible. Accordingly, in determining the ACs of **1** and **2**, conformational analysis of these molecules is simultaneously accomplished.

Results

Spiropentylcarboxylic Acid Methyl Ester, 1. The ester moiety C1C4O5O6C7 is expected to be planar with either cis or trans conformations of O5C4O6C7. Rotation can take place around the C1C4 bond. We have calculated the variation in energy of **1** as a function of the dihedral angle O5C4C1H8 for both cis and trans geometries (O5C4O6C7 $\approx 0^\circ$ and 180° , respectively) using B3LYP and the TZ2P basis set. The results, plotted in Figure 1, show that the trans geometry is uniformly >8 kcal/mol higher in energy than the cis geometry and is therefore not significantly populated at room temperature. Two stable conformations are predicted for the cis geometry. B3LYP/TZ2P optimizations lead to structures and energies for these conformations. The two conformations **1a** and **1b** differ in energy by 1.02 kcal/mol. In **1a**, the more stable conformation, the plane of the C4O5O6C7 moiety is approximately perpendicular to the plane of the adjacent cyclopropyl ring; the C=O group (C4O5) is oriented toward the cyclopropyl ring. In **1b**, the less stable conformation, the C4O5O6C7 moiety is rotated by approximately 180° , so that the C=O group is oriented away from the cyclopropyl ring. At room temperature, both **1a** and **1b** can be expected to be significantly populated, **1a** being present in higher percentage. The

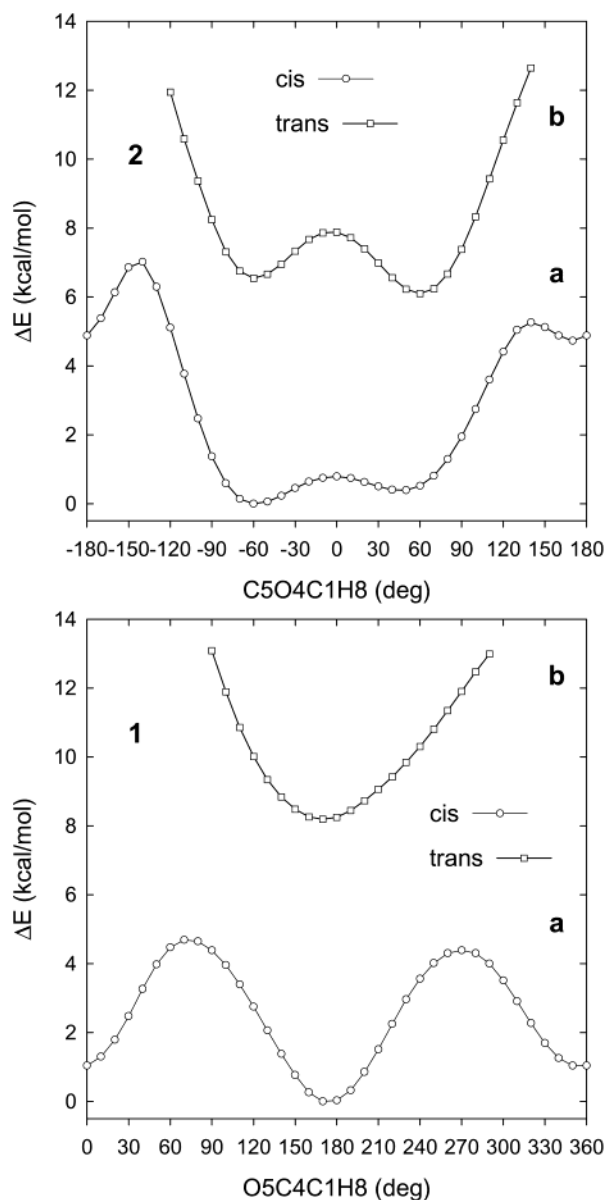


FIGURE 1. (1) B3LYP/TZ2P energy of (*R*)-**1** as a function of the dihedral angle O5C4C1H8: (a) O5C4O6C7 $\approx 0^\circ$; (b) O5C4O6C7 $\approx 180^\circ$. (2) B3LYP/TZ2P energy of (*R*)-**2** as a function of the dihedral angle C5O4C1H8: (a) C1O4C5O6 $\approx 0^\circ$; (b) C1O4C5O6 $\approx 180^\circ$.

structures of **1a** and **1b** are shown in Figure 2. Key structural parameters are given in Table 1.

The mid-IR IR and VCD spectra of **1** in CCl_4 solution are shown in Figure S1 of the Supporting Information. Analysis of these spectra is based on B3LYP/TZ2P calculations of the IR and VCD spectra of **1a** and **1b**. Predicted frequencies and dipole strengths for **1a** and **1b** are given in Table S1 of the Supporting Information. IR spectra of **1a** and **1b**, obtained thence, are shown in Figure 3, together with the conformationally averaged spectrum, obtained by summing the population-weighted spectra of **1a** and **1b**. The populations of **1a** and **1b** are calculated from the B3LYP/TZ2P energy difference via Boltzmann statistics and are 85% and 15%, respectively. The predicted spectra of **1a** and **1b** are substantially different, reflecting the substantial differences in predicted vibrational frequencies and dipole strengths. Ac-

(2) (a) Stephens, P. J.; Devlin, F. J. *Chirality* **2000**, *12*, 172. (b) Stephens, P. J.; Devlin, F. J.; Aamouche, A. In *Chirality: Physical Chemistry*; Hicks, J. M., Ed.; ACS Symposium Series 810; American Chemical Society: Washington, DC, 2002; pp 18–33.

(3) (a) Stephens, P. J.; Aamouche, A.; Devlin, F. J.; Superchi, S.; Donnoli, M. I.; Rosini, C. *J. Org. Chem.* **2001**, *66*, 3671. (b) Devlin, F. J.; Stephens, P. J.; Scafato, P.; Superchi, S.; Rosini, C. *Tetrahedron: Asymmetry* **2001**, *12*, 1551. (c) Devlin, F. J.; Stephens, P. J.; Scafato, P.; Superchi, S.; Rosini, C. *Chirality* **2002**, *14*, 1.

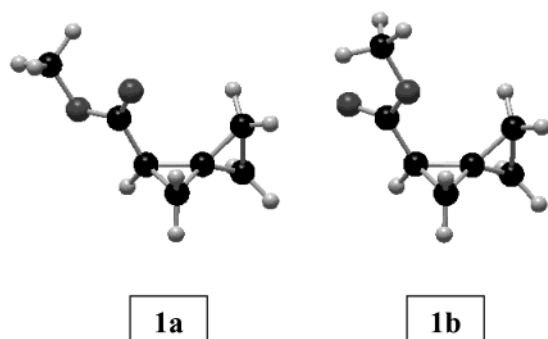


FIGURE 2. B3LYP/TZ2P structures of conformations **a** and **b** of (*R*)-**1**.

TABLE 1. B3LYP/TZ2P Dihedral Angles of the Conformations of **1** and **2**^a

	1a	1b		2a	2b
O5C4C1C2	26.4	-150.1	C5O4C1C2	158.2	99.4
O5C4C1H8	172.4	-5.5	C5O4C1H8	-58.9	46.0
O6C4C1C2	-154.1	30.3	O6C5O4C1	-0.5	-0.6
O6C4C1H8	-8.2	174.9	C7C5O4C1	178.8	179.9
C7O6C4C1	-179.6	179.6	C7C5O6O4	-179.2	179.4
C7O6C4O5	-0.1	0.0			

^a Dihedral angles in degrees for the conformations of (*R*)-**1** and (*R*)-**2**. See the text for atom numbering.

cordingly, the conformationally averaged spectrum is more complex than the individual spectra of **1a** and **1b**. Due to the much greater population of **1a**, compared to **1b**, the conformationally averaged spectrum is much closer to that of **1a** than that of **1b**. However, significant differences from the spectrum of **1a** are predicted, most dramatically in the “window” in the spectrum of **1a** between modes 32 and 33, where absorption arising from mode 32 of **1b** is prominent in the conformationally averaged spectrum.

Comparison of the conformationally averaged IR spectrum of **1** to the experimental IR spectrum leads straightforwardly to the assignment of the experimental spectrum shown in Figure 3. Bands attributable to a single fundamental of one conformation, specifically modes 15, 17, 18, 20–22, 31, and 33 of **1a** and modes 17, 18, 21–23, 32, and 33 of **1b**, are resolved, unambiguously demonstrating the presence of both conformations **1a** and **1b**. Predicted conformational splittings for modes 17 (5 cm⁻¹), 18 (12 cm⁻¹), 21 (9 cm⁻¹), 22 (11 cm⁻¹), 32 (70 cm⁻¹), and 33 (34 cm⁻¹) are in excellent agreement with the observed splittings of 6, 11, 6, 10, 72, and 37 cm⁻¹, respectively. Experimental frequencies and dipole strengths have been obtained from the experimental spectrum via Lorentzian fitting and are given in Table S1 of the Supporting Information, together with the detailed assignment of the spectrum. Experimental and calculated frequencies and dipole strengths are compared in Figure 4. Calculated frequencies are uniformly higher than experimental frequencies, the differences lying in the range 0–4%, typical of TZ2P calculations using hybrid functionals.⁴ The agreement of calculated and experimental dipole strengths is also similar to that found previously.⁴ The quantitative agreement of calculated and experimental frequencies and dipole strengths strongly supports the assignment of the IR spectrum of **1**.

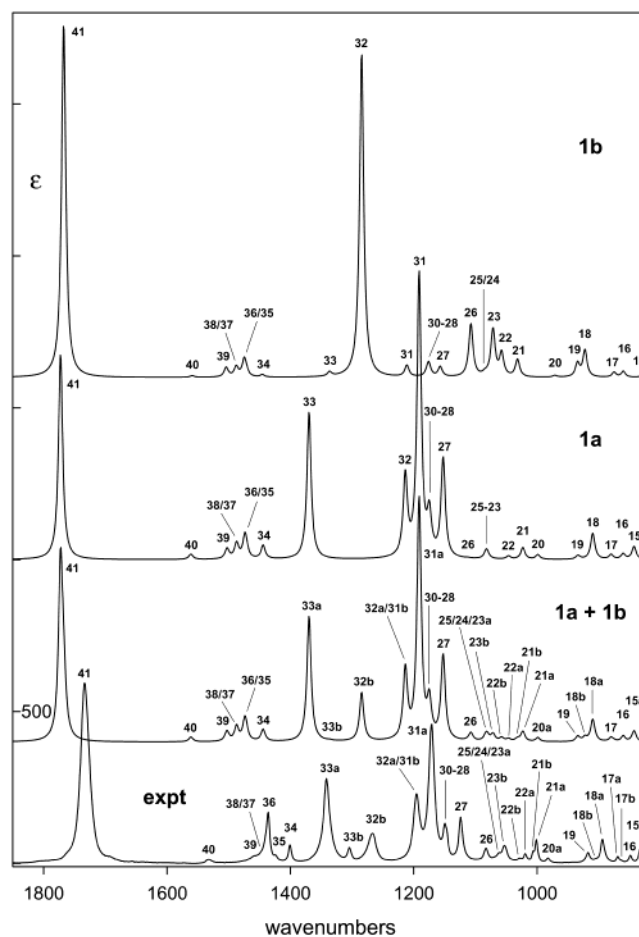


FIGURE 3. Calculated and experimental IR spectra of **1**. The calculated spectra of **1a** and **1b** are obtained from B3LYP/TZ2P frequencies and dipole strengths using Lorentzian band shapes ($\gamma = 4.0$ cm⁻¹). The spectrum of the equilibrium mixture of **1a** and **1b** is obtained using populations of **1a** and **1b** calculated from their B3LYP/TZ2P energies. Fundamentals are numbered, **a** and **b** referring to conformations **1a** and **1b**. A number alone indicates that the modes of **1a** and **1b** are not resolved. The experimental spectrum is from Figure S1 of the Supporting Information.

The rotational strengths predicted for the *R* enantiomers of **1a** and **1b** are given in Table S1 of the Supporting Information. VCD spectra obtained thence are shown in Figure 5, together with the conformationally averaged VCD spectrum. As with the IR spectra, the VCD spectra of **1a** and **1b** are very different. As a result, the conformationally averaged VCD spectrum is more complex than the individual spectra of **1a** and **1b**. Due to the much greater population of **1a**, as compared to **1b**, the conformationally averaged spectrum is much closer to that of **1a** than to that of **1b**. However, significant differences are predicted.

The conformationally averaged VCD spectrum of (*R*)-**1** is compared to the experimental spectrum of (+)-**1**, multiplied by -1, in Figure 5. The agreement is qualitatively excellent. VCD is observed for the resolved

(4) (a) Devlin, F. J.; Stephens, P. J.; Cheeseman, J. R.; Frisch, M. J. *J. Phys. Chem.* **1997**, *101*, 6322. (b) Devlin, F. J.; Stephens, P. J.; Cheeseman, J. R.; Frisch, M. J. *J. Phys. Chem.* **1997**, *101*, 9912. (c) Devlin, F. J.; Stephens, P. J. *J. Phys. Chem.* **1999**, *103*, 527. (d) Ashvar, C. S.; Devlin, F. J.; Stephens, P. J. *J. Am. Chem. Soc.* **1999**, *121*, 2836. (e) Devlin, F. J.; Stephens, P. J. *J. Am. Chem. Soc.* **1999**, *121*, 7413.

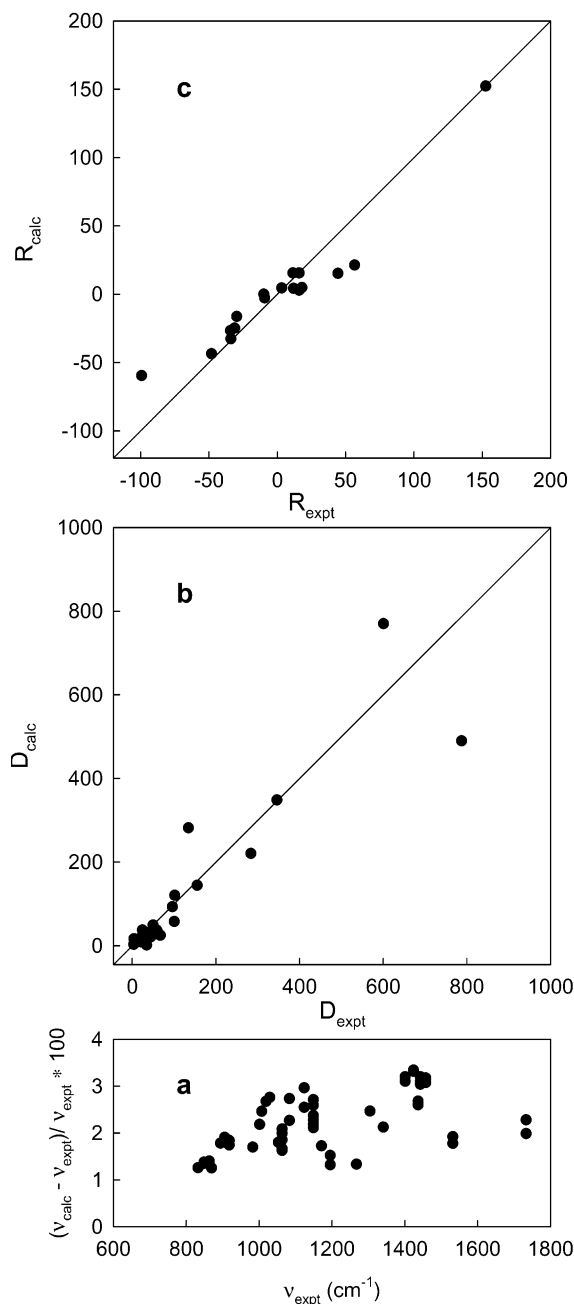


FIGURE 4. Comparison of calculated and experimental frequencies (a), dipole strengths (b), and rotational strengths (c) for **1**. Calculated dipole and rotational strengths are the population-weighted averages of the dipole and rotational strengths of **1a** and **1b**. Calculated rotational strengths are for (*R*)-**1**. Experimental rotational strengths are for (+)-**1**, multiplied by -1 , and are normalized to 100% ee. Frequencies, dipole strengths, and rotational strengths are in cm^{-1} , $10^{-40} \text{esu}^2 \text{cm}^2$, and $10^{-44} \text{esu}^2 \text{cm}^2$, respectively.

fundamentals 15, 17, 18, 20–22, and 33 of **1a** and 23 and 32 of **1b**. The excellence of the qualitative agreement of the predicted VCD spectrum for (*R*)-**1** with the mirror image of the experimental VCD for (+)-**1** leads to the unambiguous conclusion that the AC of **1** is *R*(–)/*S*(+). Experimental and calculated rotational strengths, the former corrected to 100% ee, are compared in Figure 4. The agreement is comparable to that found previously for TZ2P calculations of rotational strengths using hybrid

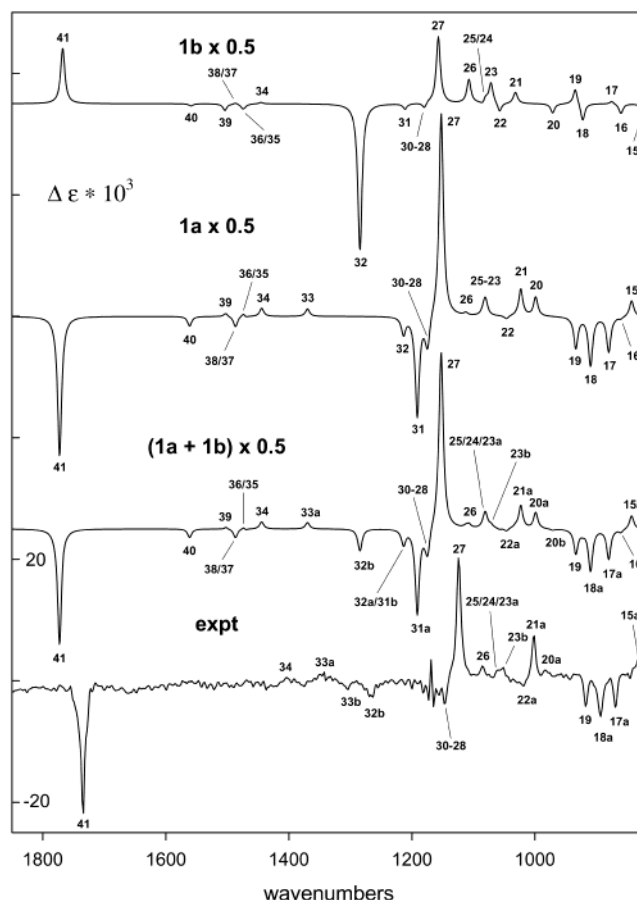


FIGURE 5. Calculated and experimental VCD spectra of **1**. The calculated spectra of **1a** and **1b** are obtained from the B3LYP/TZ2P frequencies and rotational strengths of (*R*)-**1** using Lorentzian band shapes ($\gamma = 4.0 \text{ cm}^{-1}$). The spectrum of the equilibrium mixture of **1a** and **1b** is obtained using populations of **1a** and **1b** calculated from their B3LYP/TZ2P energies. Fundamentals are numbered, **a** and **b** referring to conformations **1a** and **1b**. A number alone indicates that the modes of **1a** and **1b** are not resolved. The experimental spectrum is that in Figure S1 of the Supporting Information, multiplied by -1 .

functionals.⁴ The quantitative agreement between theory and experiment further confirms the assignment of the AC of **1** and, in addition, strongly supports the assignment of the VCD spectrum of **1**.

Spiropentyl Acetate, 2. The acetate moiety C1O4C5O6C7 is expected to be planar with either cis or trans conformations of O4C5O6C7. Rotation can take place around the C1O4 bond. We have calculated the variation in energy of **2** as a function of the dihedral angle C5O4C1H8 for both the cis and trans geometries (C1O4C5O6 $\approx 0^\circ$ and 180° , respectively) using B3LYP and the TZ2P basis set. The results, plotted in Figure 1, show that the trans geometry is uniformly $>5 \text{ kcal/mol}$ higher in energy than the cis geometry and is therefore not significantly populated at room temperature. Three stable conformations are predicted for the cis geometry. B3LYP/TZ2P optimizations lead to structures and energies for these conformations. Two conformations, **2a** and **2b**, differ in energy by 0.38 kcal/mol. In these conformations the acetate group is rotated by $\sim 57^\circ$ and $\sim 45^\circ$ relative to the geometry in which the plane of the acetate group is perpendicular to the plane of the adjacent

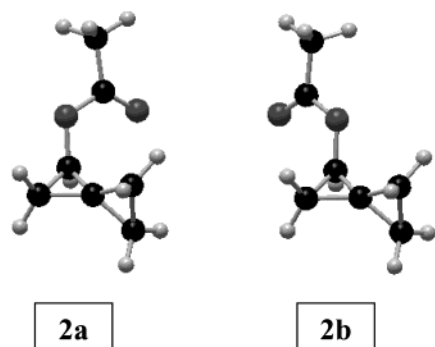


FIGURE 6. B3LYP/TZ2P structures of conformations **a** and **b** of (*R*)-**2**.

cyclopropyl ring, with the C=O group oriented away from the cyclopropyl group. A third conformation, **2c**, lies >4 kcal/mol higher in energy than **2a**. In **2c**, the planes of the acetate and cyclopropyl groups are nearly perpendicular, with the C=O group oriented toward the cyclopropyl group. At room temperature, **2a** and **2b** can be expected to be significantly populated, but not **2c**. The structures of **2a** and **2b** are shown in Figure 6. Key structural parameters of **2a** and **2b** are given in Table 1.

The mid-IR IR and VCD spectra of **2** in CCl₄ solution are shown in Figure S2 of the Supporting Information. Analysis of these spectra is based on B3LYP/TZ2P calculations of the IR and VCD spectra of **2a** and **2b**. Predicted frequencies and dipole strengths for **2a** and **2b** are given in Table S2 of the Supporting Information. IR spectra of **2a** and **2b**, obtained thence, are shown in Figure 7, together with the conformationally averaged spectrum, obtained by summing the population-weighted spectra of **2a** and **2b**. The populations of **2a** and **2b** are calculated from the B3LYP/TZ2P energy difference via Boltzmann statistics and are 66% and 34%, respectively. The predicted spectra of **2a** and **2b** are quite similar. The largest differences are observed for fundamentals 19/20 and 27/28. The predicted conformationally averaged IR spectrum is very similar to the spectra of **2a** and **2b**, therefore; qualitative differences are observed only for modes 19/20 and 27/28.

Assignment of the experimental IR spectrum of **2** is straightforward as shown in Figure 7. The presence of conformations **2a** and **2b** is clearly shown by the resolution of fundamentals 19 and 28 of **2a** and **2b**. Experimental frequencies and dipole strengths have been obtained from the experimental spectrum via Lorentzian fitting and are given in Table S2 of the Supporting Information, together with the detailed assignment of the spectrum. Experimental and calculated frequencies and dipole strengths are compared in Figure 8. Calculated frequencies are uniformly higher than experimental frequencies, the differences lying in the range 0–4%, typical of TZ2P calculations using hybrid functionals.⁴ The agreement of calculated and experimental dipole strengths is also similar to that found previously.⁴ The quantitative agreement of calculated and experimental frequencies and dipole strengths strongly supports the assignment of the IR spectrum of **2**.

The rotational strengths predicted for the *R* enantiomers of **2a** and **2b** are given in Table S2 of the Supporting Information. VCD spectra obtained thence are shown in Figure 9, together with the conformationally

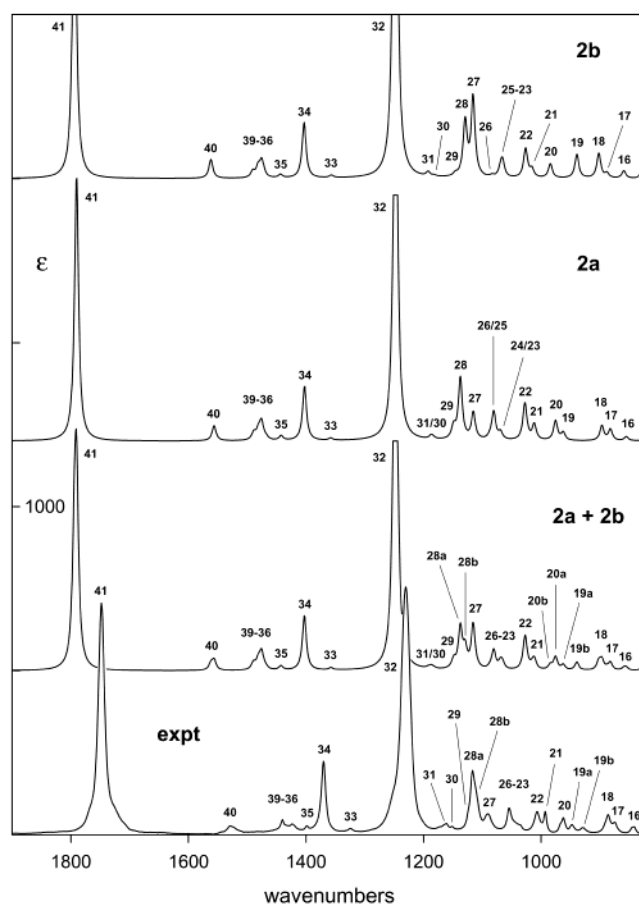


FIGURE 7. Calculated and experimental IR spectra of **2**. The calculated spectra of **2a** and **2b** are obtained from B3LYP/TZ2P frequencies and dipole strengths using Lorentzian band shapes ($\gamma = 4.0 \text{ cm}^{-1}$). The spectrum of the equilibrium mixture of **2a** and **2b** is obtained using populations of **2a** and **2b** calculated from their B3LYP/TZ2P energies. Fundamentals are numbered, **a** and **b** referring to conformations **2a** and **2b**. A number alone indicates that the modes of **2a** and **2b** are not resolved. The experimental spectrum is from Figure S2 of the Supporting Information.

averaged spectrum. In contrast to the IR spectra of **2a** and **2b**, the VCD spectra show little similarity. As a result, the conformationally averaged VCD spectrum is substantially different from the spectra of both **2a** and **2b**. The differences are predominantly differences in intensity; as in the case of the IR spectrum, additional bands, due to frequency differences in the modes of **2a** and **2b**, are only observed to a limited extent.

The conformationally averaged VCD spectrum of (*R*)-**2** is compared to the experimental spectrum of (+)-**2** in Figure 9. The agreement is qualitatively excellent. Positively signed VCD predicted for fundamental 19 of **2a** and **2b** is clearly observed, further confirming the presence of both **2a** and **2b**. Only in the case of fundamental 21 are the predicted and experimental VCDs in qualitative disagreement: the predicted VCD is negatively signed, while the observed VCD is positively signed. The excellence of the qualitative agreement of the predicted VCD spectrum for (*R*)-**2** with the experimental VCD for (+)-**2** leads to the unambiguous conclusion that the AC of **2** is *R*(+)/*S*(-). Experimental rotational strengths have been obtained from the experimental VCD spectrum via Lorentzian fitting and are given in Table S2 of the

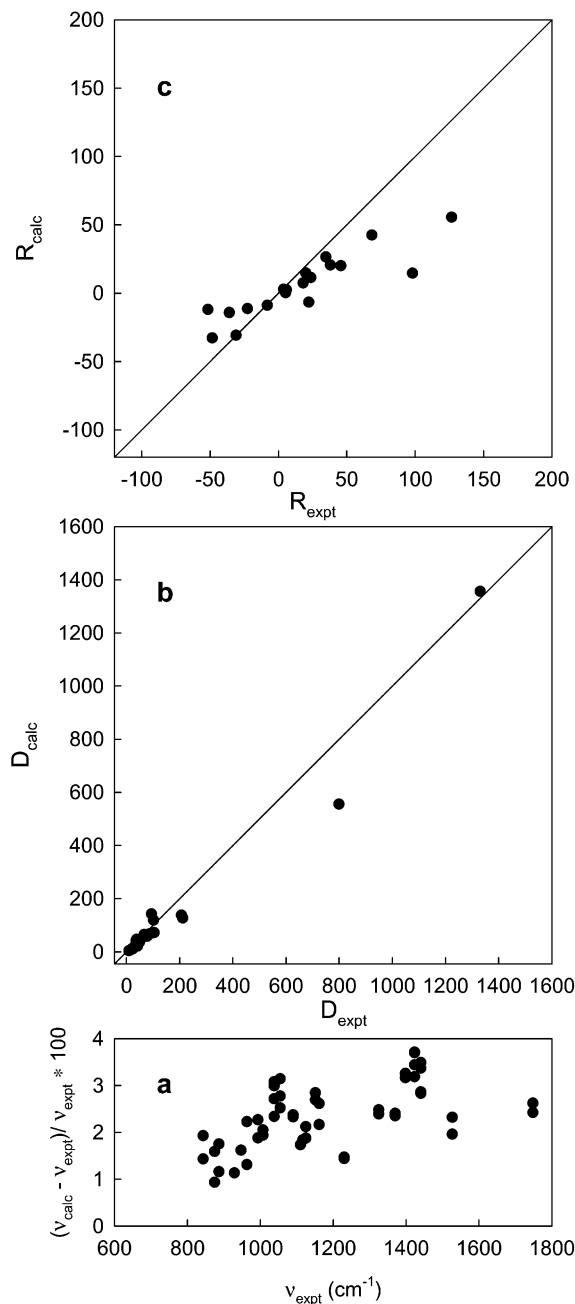


FIGURE 8. Comparison of calculated and experimental frequencies (a), dipole strengths (b), and rotational strengths (c) for **2**. Calculated dipole and rotational strengths are the population-weighted averages of the dipole and rotational strengths of **2a** and **2b**. Calculated rotational strengths are for (*R*)-**2**. Experimental rotational strengths are for (+)-**2** and are normalized to 100% ee. Frequencies, dipole strengths, and rotational strengths are in cm^{-1} , $10^{-40} \text{ esu}^2 \text{ cm}^2$, and $10^{-44} \text{ esu}^2 \text{ cm}^2$, respectively.

Supporting Information. Comparison to calculated rotational strengths is shown in Figure 8. The agreement is comparable to that found previously for TZ2P calculations of rotational strengths using hybrid functionals.⁴ The quantitative agreement between theory and experiment further confirms the assignment of the AC of **2** and, in addition, strongly supports the assignment of the VCD spectrum of **2**.

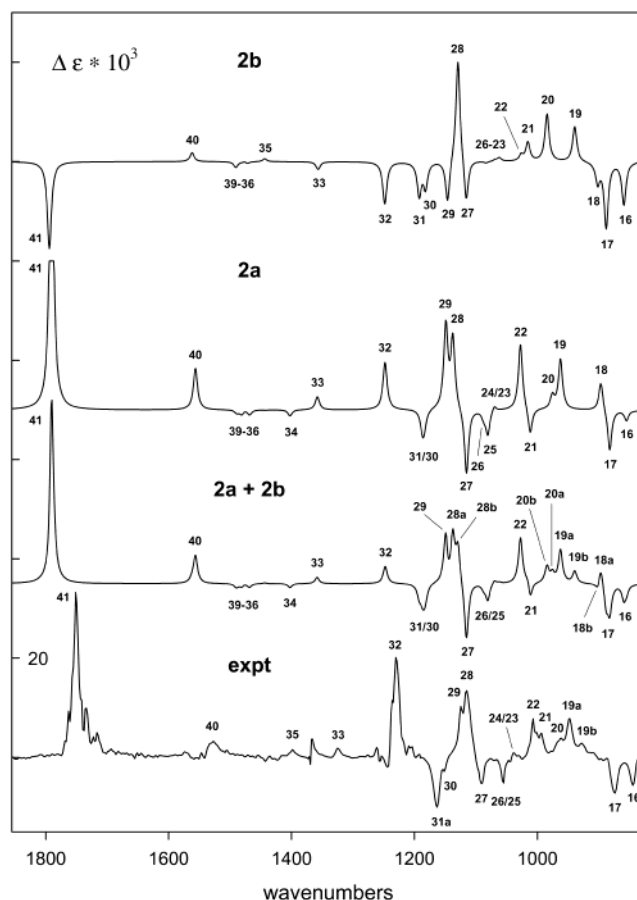


FIGURE 9. Calculated and experimental VCD spectra of **2**. The calculated spectra of **2a** and **2b** are obtained from the B3LYP/TZ2P frequencies and rotational strengths of (*R*)-**2** using Lorentzian band shapes ($\gamma = 4.0 \text{ cm}^{-1}$). The spectrum of the equilibrium mixture of **2a** and **2b** is obtained using populations of **2a** and **2b** calculated from their B3LYP/TZ2P energies. Fundamentals are numbered, **a** and **b** referring to conformations **2a** and **2b**. A number alone indicates that the modes of **2a** and **2b** are not resolved. The experimental spectrum is from Figure S2 of the Supporting Information.

Discussion

The principal goal of this work was to determine the ACs of the spiroentyl derivatives **2** and **4** using VCD spectroscopy. VCD measurements are typically carried out using solution concentrations in the range 0.01–1 M.² At such concentrations, aggregation of carboxylic acids occurs. Aggregation can substantially perturb VCD spectra.⁵ Accordingly, instead of studying **4** directly, we have studied its methyl ester, **1**. Aggregation is not anticipated in either **1** or **2**.

The IR and VCD spectra of **1** and **2** have been studied in CCl_4 solution in the mid-IR spectral region. The use of CCl_4 has two advantages: (1) absorption in the mid-IR is limited; (2) solute–solvent interactions are minimized. Analysis of the IR and VCD spectra of **1** and **2** has been based on B3LYP/TZ2P DFT calculations. The hybrid functional B3LYP is a state-of-the-art functional.⁶ The TZ2P basis set provides IR and VCD spectra close to complete basis set limit spectra.^{2b} The principal error

(5) Nafie, L. A.; Keiderling, T. A.; Stephens, P. J. *J. Am. Chem. Soc.* **1976**, *98*, 2715.

in our calculations is the neglect of anharmonicity, as a result of which calculated vibrational frequencies are higher than experimental frequencies by a few percent.⁷

In both **1** and **2** DFT calculations predict two stable conformations which can be expected to be populated at room temperature. In **1**, these two conformations correspond to the two possible orientations of the (cis) ester group, with its plane perpendicular to that of the adjacent cyclopropyl ring. This perpendicular orientation is preceded in substituted cyclopropanes. Carbonyl-substituted cyclopropanes adopt such a conformation to maximize the overlap of the carbon p-orbital of the carbonyl group with the cyclopropane bent bonds.⁸ The structure of the lower energy conformation of **1**, **1a**, corresponds to that of the lower energy conformer of cyclopropanecarboxylic acid.^{8b} A reason for the lower energy of **1a** may be found in the O–C nonbonded distance. With **1a**, the distances from the carbonyl oxygen to the ring carbons are calculated to be 2.976 and 3.025 Å, whereas with **1b** the distances from the ether oxygen to the carbons are shorter, 2.892 and 2.926 Å.

In **2**, there are three conformations of the (cis) acetate group; two are of energies permitting population at room temperature. The acetate groups in these latter conformations are rotated in opposite directions from the structure in which the plane of the acetate group is perpendicular to the plane of the adjacent cyclopropyl group, with the C=O moiety oriented away from the cyclopropyl ring. The energy difference of these two conformations is quite small (~0.4 kcal/mol). The spiro-pentyl acetates **2a** and **2b** correspond to the gauche conformer of cyclopropanol, which is known to be the low-energy form.⁹ The calculated difference in energy is quite small, and is difficult to rationalize.

The IR spectra of **1** and **2** predicted by B3LYP/TZ2P calculations are in excellent agreement with the experimental IR spectra of **1** and **2**, allowing for the overall shift of the predicted spectra to higher frequency due to the neglect of anharmonicity.⁷ In particular, unequivocal evidence of the two conformations predicted by DFT is provided: bands are clearly resolved in the spectrum of **1** assignable to either **1a** or **1b**; likewise, in the spectrum of **2**, bands of either **2a** or **2b** are clearly assignable. As a result, we can confidently assign the IR spectra of **1** and **2**. Further, the excellent agreement of predicted and experimental frequencies and dipole strengths demonstrates the reliability of the calculated spectra and, hence, of the conformational structures predicted by DFT.

The ACs of **1** and **2** are determined by comparison of predicted and experimental VCD spectra. Predicted VCD spectra are in excellent agreement with experiment in sign and magnitude when the predicted spectrum for (*R*)-**1** is compared to the experimental spectrum for (+)-**1**, multiplied by –1, and when the predicted spectrum for (*R*)-**2** is compared to the experimental spectrum for

(+)-**2**. The ACs of **1** and **2** are thus unambiguously *R*(–)/*S*(+) and *R*(+)/*S*(–), respectively. The AC reported earlier for **2** was *R*(+)/*S*(–).¹ The AC reported earlier for **4** was *R*(–)/*S*(+).¹ (+)-**4** yields (+)-**1**. The ACs deduced from the VCD of **1** and **2** are thus consistent with those reported earlier for **4** and **2**, which resulted from X-ray crystallography of the α-phenylethylammonium salt of **4**.¹ Our results confirm the reported identification of the NH₃⁺ and CH₃ groups of the α-phenylethylammonium ion in the X-ray structure.

Methods

Spiropentylcarboxylic acid methyl ester, **1**, and spiro-pentyl acetate, **2**, were synthesized from spiro-pentylcarboxylic acid, **4**. Racemic **4** was prepared by rhodium-catalyzed addition of ethyl diazoacetate to methylenecyclopropane, followed by hydrolysis.¹⁰ Resolution of racemic **4** was carried out via fractional crystallization from ethyl acetate of salts of either (–)-brucine or (–)-α-phenylethylamine, as described previously.¹ (–)-**4** with [α]_D = –172.7° (MeOH) was earlier shown¹ to have an ee of 95.5%, leading to a maximum rotation of –180.8° (MeOH). The ester **1** was prepared from **4** using diazomethane in ether. (+)-**1** was obtained from (+)-**4**, resolved using (–)-brucine, of [α]_D = +63.6° (MeOH) and 35.2% ee. The [α]_D²⁵ of (+)-**1** in CCl₄ (*c* = 1.46) was 67.4°. The acetate **2** was prepared from **4** via conversion to the methyl ketone using methylolithium, followed by Baeyer–Villiger oxidation using urea/hydrogen peroxide and trifluoroacetic anhydride, as described previously.¹ (+)-**2** was obtained from (–)-**4**, resolved using (–)-α-phenylethylamine, of [α]_D = –116° (MeOH) and ee 64.2% ee. The [α]_D²⁵ of (+)-**2** in CCl₄ (*c* = 3.15) was 27.5°.

IR spectra were measured at 1 cm^{–1} resolution. VCD spectra were measured at 4 cm^{–1} resolution. VCD scans were 1 h long. IR and VCD spectra of CCl₄ solutions of **1** and **2** were measured using KBr cells. The VCD spectra of racemic **1** and **2** provided the baselines for the spectra of (+)-**1** and (+)-**2**, respectively. Experimental frequencies, dipole strengths, and rotational strengths were obtained from experimental IR and VCD spectra via Lorentzian fitting.^{4a,b}

Ab initio DFT calculations using the functional B3LYP^{11,12} and the basis set TZ2P¹³ were carried out using Gaussian 98.¹⁴ All calculations used analytical derivative methods and perturbation-dependent basis sets. Harmonic vibrational frequencies, dipole strengths, and rotational strengths were obtained from Hessians, atomic polar tensors (APT), and atomic axial tensors (AATs). IR and VCD spectra were further obtained using Lorentzian band shapes.

Acknowledgment. This work has been supported by an NSF grant (CHE-9903832) to P.J.S. and an NSF grant (CHE-9707677) to K.B.W. Computer time at the USC Research Computing Facility is gratefully acknowledged.

Supporting Information Available: B3LYP/TZ2P-optimized geometries and total energies, frequencies, dipole strengths, and rotational strengths for structures **1a**, **1b**, **2a**, and **2b**, and IR and VCD spectra for **1** and **2**. This material is available free of charge via the Internet at <http://pubs.acs.org>.

JO020225N

(6) Frisch, M. J.; Trucks, G. W.; Cheeseman, J. R. In *Recent Developments and Applications of Modern Density Functional Theory: Theoretical and Computational Chemistry*; Seminario, J. M., Ed.; Elsevier: New York, 1996; Vol. 4, p 679.

(7) Finley, J. W.; Stephens, P. J. *J. Mol. Struct.: THEOCHEM* **1995**, 357, 225.

(8) (a) Cyclopropanecarboxaldehyde: Durig, J. R.; Fing, F.; Little, T. S.; Wang, A. Y. *Struct. Chem.* **1992**, 3, 417. (b) Cyclopropanecarboxylic acid: Marstokk, K. M.; Moellendal, H.; Samdal, S. *Acta Chem. Scand.* **1991**, 45, 37.

(9) Macdonald, J. N.; Norbury, D.; Sheridan, J. *J. Chem. Soc., Faraday Trans. 2* **1978**, 74, 1365.

(10) de Meijere, A.; Kozhuskov, S. I.; Spaeth, T.; Zefirov, N. S. *J. Org. Chem.* **1993**, 58, 502.

(11) Stephens, P. J.; Devlin, F. J.; Chabalowski, C. F.; Frisch, M. J. *J. Phys. Chem.* **1994**, 98, 11623.

(12) Becke, A. D. *J. Chem. Phys.* **1993**, 98, 1372, 5648.

(13) Stephens, P. J.; Jalkanen, K. J.; Amos, R. D.; Lazzeretti, P.; Zanasi, R. *J. Phys. Chem.* **1990**, 94, 1811.

(14) Frisch, M. J.; et al. *Gaussian 98*; Gaussian Inc.: Pittsburgh, Pa.